Performance Report

November 28, 1988 - Feb. 27, 1989

Sixth Quarter (Three Months)

Contract DAAB07-87-C-FO94

With the U.S. Army Night Vision and Electro-Optics Center

Fort Belvoir, Virginia 22060-5677

Contract Monitor: Mr. Fred Carlson

"Two-Photon Absorption Characterization"

Principal Investigators:

Dr. Chris L. Littler

Dr. David G. Seiler

Department of Physics

University of North Texas

Denton Texas, 76203

The views, opinions, and/or findings contained in this report are those of the authors and should not be construed as an official Department of the Army position, policy, or decision, unless designated by other documentation.

Unclassified

SECURITY CLASSIFICATION OF THIS PAGE

REPORT DOCUMENTATION PAGE

Form Approved OMB No 0704-0188

1a. REPORT SECURITY CLASSIFICATION Unclassified	1b RESTRICTIVE MARKINGS
2a. SECURITY CLASSIFICATION AUTHORITY	3. DISTRIBUTION/AVAILABILITY OF REPORT Approved for public release; Distribution is Unlimited
2b. DECLASSIFICATION/DOWNGRADING SCHEDULE	
4. PERFORMING ORGANIZATION REPORT NUMBER(S) NA	5. MONITORING ORGANIZATION REPORT NUMBER(S) NA
6a. NAME OF PERFORMING ORGANIZATION Univ. of North Texas; 6b. OFFICE SYMBOL (If applicable)	7a. NAME OF MONITORING ORGANIZATION Center for Night Vision and Electro-Optics
6c. ADDRESS (City, State, and ZIP Code)	7b. ADDRESS (City, State, and ZIP Code) ATTN: AMSEL-RD-NV-IRT Fort Belvoir, VA 22060-5677
8a. NAME OF FUNDING/SPONSORING ORGANIZATION CNVEO; 8b. OFFICE SYMBOL (If applicable) AMSEL-RD-NV-IT	9 PROCUREMENT INSTRUMENT IDENTIFICATION NUMBER DAAB07-87-C-F094
8c. ADDRESS (City, State, and ZIP Code) Fort Belvoir, VA 22060-5677	10 SOURCE OF FUNDING NUMBERS

PROGRAM ELEMENT NO.	PROJECT NO.	TASK NO	WORK UNIT ACCESSION NO
661102A	1L161102A31B	HO	007-CJ

11. TITLE (Include Security Classification)

Two Photon Characterization

12. PERSONAL AUTHOR(S)

Chris Littler

13a. TYPE OF REPORT	13b. TIME COVERED	14. DATE OF REPORT (Year, Month, Day)	15 PAGE COUNT
Interim	FROM 11/88 TO 2/89	89/5/15	13

16. SUPPLEMENTARY NOTATION

17. COSATI CODES		
FIELD	GROUP	SUB-GROUP
17	05	

18. SUBJECT TERMS (Continue on reverse if necessary and identify by block number)

Defect characterization, Magneto-Optical measurements, Two Photon Spectroscopy, Narrow band gap semiconductors. II-VI compounds.

19. ABSTRACT (Continue on reverse if necessary and identify by block number)

Magneto-Optical measurements of $Hg_{1-x}Cd_xTe$ alloys have provided a new means of studying impurities and defects in this important II-VI material. Two-photon magnetoabsorption (TMPA) has been used to accurately determine the temperature dependence of the energy gap of various HgCdTe alloys, revealing behavior that deviates from currently accepted models. In addition, magneto-optical techniques have been used to detect the presence of both shallow and deep impurities/defects and accurately determine their activation energies, thus providing information necessary for understanding the electrical and optical properties of the material.

20. DISTRIBUTION/AVAILABILITY OF ABSTRACT ☐ UNCLASSIFIED/UNLIMITED ☒ SAME AS RPT. ☐ DTIC USERS	21. ABSTRACT SECURITY CLASSIFICATION Unclassified
22a. NAME OF RESPONSIBLE INDIVIDUAL Frederick F. Carlson	22b. TELEPHONE (Include Area Code) 703-664-5036; 22c. OFFICE SYMBOL AMSEL-RD-NV-IT

DD Form 1473, JUN 86 — Previous editions are obsolete

SECURITY CLASSIFICATION OF THIS PAGE

Unclassified

Performance Report
November 28, 1988 - Feb. 27, 1989
Sixth Quarter (Three Months)

Contract DAAB07-87-C-FO94

"Two-Photon Absorption Characterization"

Principal Investigators:
Dr. Chris L. Littler
Dr. David G. Seiler
University of North Texas

According to the Time Phase Task Schedule for the sixth quarter on p. 26 of the proposed technical work, our research investigation and sample characterization has proceeded along the two task categories (b) and (c):

(b) Investigate two-photon absorption...

(c) Identify impurity-related energy levels and correlate...

We shall now address the progress in each of the tasks.

I. (b) Investigate Two-Photon Absorption

During this quarter, we have worked on extending the two-photon absorption technique to the study of lower x- value samples. Particularly, we have started to study samples with x = 0.23 and lower, since these have 77 K cutoff wavelengths in the 10 - 14 μm wavelength range. Some of the samples that we have investigated in this x-value range show a wealth of impurity-related magneto-optical structure. The results from one such sample will be presented in this report.

The electrical data from two new samples studied this quarter are given below.

n-HgCdTe (x=0.224) (sample # 2)

This sample was grown by Texas Instruments (TI) using the traveling heater method (THM). It had the following properties:

$$\mu\,(77K) \simeq 1 \times 10^5 \frac{cm^2}{V\text{-}sec}$$
$$n\,(77K) \simeq 5 \times 10^{14}\ cm^{-3}$$
$$E_g\ (77K) = 120\ meV$$

n-HgCdTe (x=0.294) (Sample # 9)

This sample was grown by TI using solid state recrystallization techniques. It had the following properties:

$$\mu\,(77K) = 4.3 \times 10^5 \frac{cm^2}{V\text{-}sec}$$
$$n\,(77K) = 3.5 \times 10^{15}\ cm^{-3}$$
$$E_g\ (77K) = 243\ meV$$

Figures 1-8 show the data and analysis of samples # 2, 6, 9, and 10 (the details on the electrical properties are given in Table 1). For each sample, two-photon magnetoabsorption (TPMA) was observed and analyzed. The energy gap of each sample was determined from these measurements and this information was used to to reference the activation energies of the impurity and defect levels discussed in the next section. As can be seen from the data in Figure 2, Sample # 2 has an energy gap of 99 meV (at 7K) . This translates to a 77K gap of $\simeq$ 120 meV, or a cutoff wavelength of $\simeq$ 10.3 μm. Thus, twe can clearly use TPMA measurements to investigate samples with cutoff wavelengths in the 8-10 μm wavelength regoin. In addition to TPMA, we also observe magneto-optical resonances from impurity/defect levels. This data will be discussed in the next section of this report.

Since TPMA techniques have been well established, one of the main thrusts in the sixth quarter was on the investigation of the impurity-related magnetoabsorption, using TPMA as a tool to aid in the delineation of impurity and interband absorption processes. We now discuss these results.

II. c. Identify impurity-related levels and correlate...

In past reports we have shown initial measurement of impurity and defect levels in HgCdTe. These results showed that, using magneto-optical techniques, it was possible to measure both shallow acceptor levels and midgap states. As a result of these initial measurements we concentrated this quarter on obtaining an extensive set of impurity magneto-optical data in order to develop a clearer picture of what levels are present and thus how they might impact detector performance. Figure 1 shows impurity magneto-optical (IMO) spectra from sample #2. As indicated by the downward pointing arrows, only one TPMA resonance is observed at the highest magnetic field and the longest CO_2 laser wavelength. However, as indicated by the upward pointing arrows, there is a wealth of weaker magneto-optical resonances. Figure 2 shows the results of analyzing this data using the Pidgeon-Brown energy band model. The band model was used to calculate the energy gap and the activation energy of impurity and defect levels. A 1/4 waveplate was used to check the polarization dependence of all transitions and verify our identification of the nature of the transitions. From the comparison of theory and experimental data for sample # 2, the impurity and defect activation energies in sample # 2 are 18 and 26 meV above the valence band, respectively. For the calculation of the activation energy, the transition energies from the impurity or defect levels to the conduction band via one-photon absorption can be described by the relationship

$$\hbar\omega = E_C (n,B) - E_i,$$

where E_i is the energy of the identified level (midgap, shallow acceptor, etc.) above the valence band. As $B \rightarrow 0$, $E_C (n,B) \rightarrow E_g$ and thus

$$\hbar\omega = E_g - E_i,$$

which is the B=0 intercept.

Figure 3 shows the wavelength dependence of PC response of sample # 6. Magneto-optical structure located at low field are identified as arising from midgap states. Figure 4 shows the comparison between theoritical predictions and magneto-optical absorption data, yielding the energy gap of 136 meV and the activation energies of 63 and 68 meV at T = 7K. In Figures 5 and 7 the wavelength dependence of PC response of samples #9 and 10 (# 10 is p-type) both TPMA and midgap levels were identified. Figures 6 and 8 show the comparison between theoretical predictions and magneto-optical data and the midgap levels located at 111.5 and 116.0 meV and 108 and 113 meV above the valence band, respectively. The complete results and analysis for 10 samples of different x values are summarized in Table 1. To summarize, we have observed the presence of at at least three impurity/defect levels in HgCdTe: (1) a shallow acceptor level located about 10-12 meV above the valence band whose binding energy is independent of E_g, (2) two levels located approximately at midgap (1/2 E_g), and (3) levels whose energies translate to $\simeq 0.25\ E_g$ above the valence band.

Table 1. Sample Properties and Magneto-Optical Results

No.	n(77K) (cm^{-3})	μ(77K) $\left(\frac{cm^2}{Vs}\right)$	E_g(7K) (meV)	X	E_1 shallow acceptor	E_2 Midgap Levels	E_3
1	n, $\simeq 5x10^{14}$	$\propto 1x10^5$	80.0	0.215	10.0	-	-
2	n, $\simeq 5x10^{14}$	$\propto 1x10^5$	99.0	0.224	18.0	26.0	-
3	n, $1.4x10^{14}$	$1.6x10^5$	122.0	0.237	9.8	-	-
4	n, $2.8x10^{14}$	$1.2x10^5$	125.0	0.239	10.0	60.0	-
5	n, $2.3x10^{14}$	$1.3x10^5$	136.0	0.245	10.4	-	-
6	n, $\simeq 5x10^{14}$	$\propto 1x10^5$	136.0	0.245	-	63.0	68.0
7	n, $\simeq 5x10^{14}$	$\propto 1x10^5$	136.0	0.245	12.0	18.0	-
8	n, $1.4x10^{14}$	$6.5x10^4$	188.0	0.276	-	90.0	94.0
9	n, $3.5x10^{14}$	$4.3x10^5$	222.0	0.294	-	116.0	111.5
10	p, $1.5x10^{15}$	500.0	225.0	0.298	-	108.0	113.0

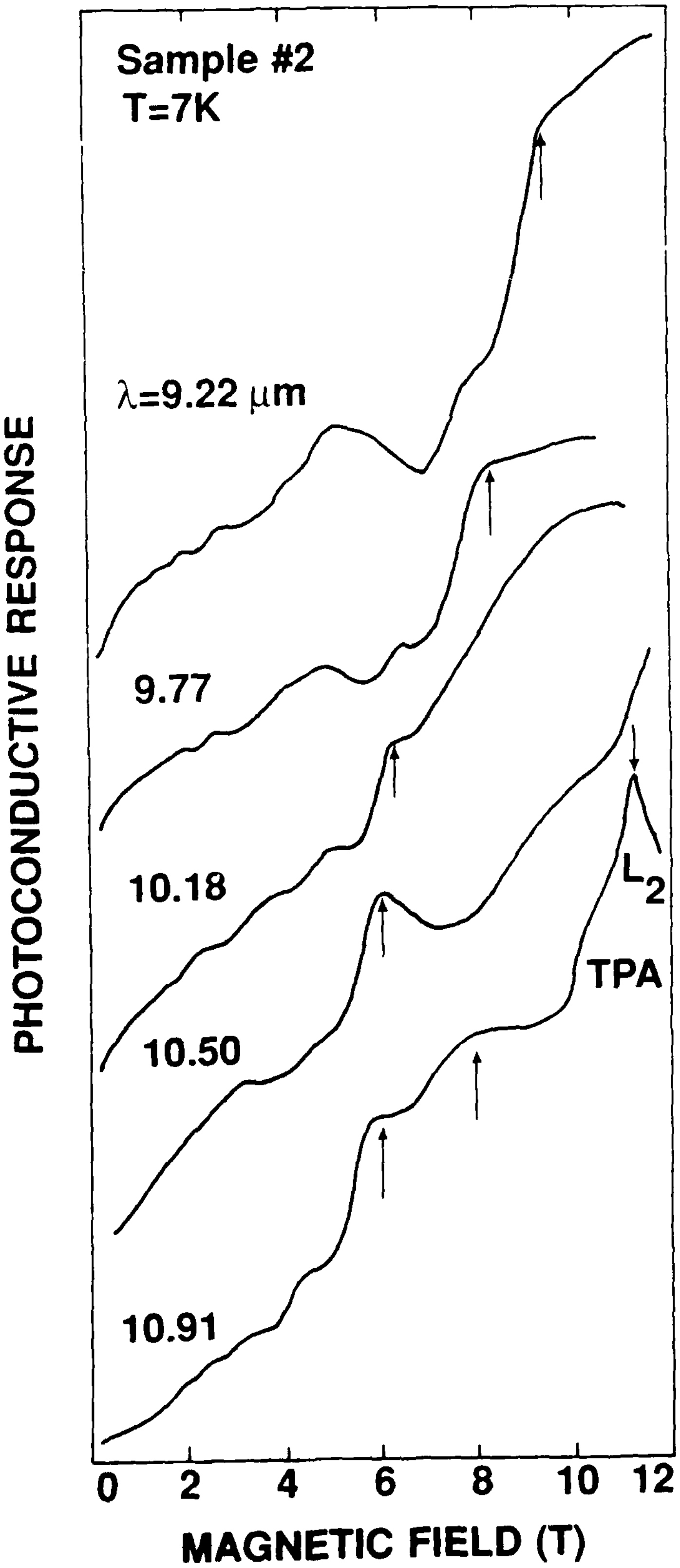

Figure 1. Wavelength dependence of the photoconductive (PC) response for sample 2. At high fields and long wavelengths TPMA resonant structure is seen (downward arrow); at lower fields transitions from deep levels to the conduction band (up arrows) are observed.

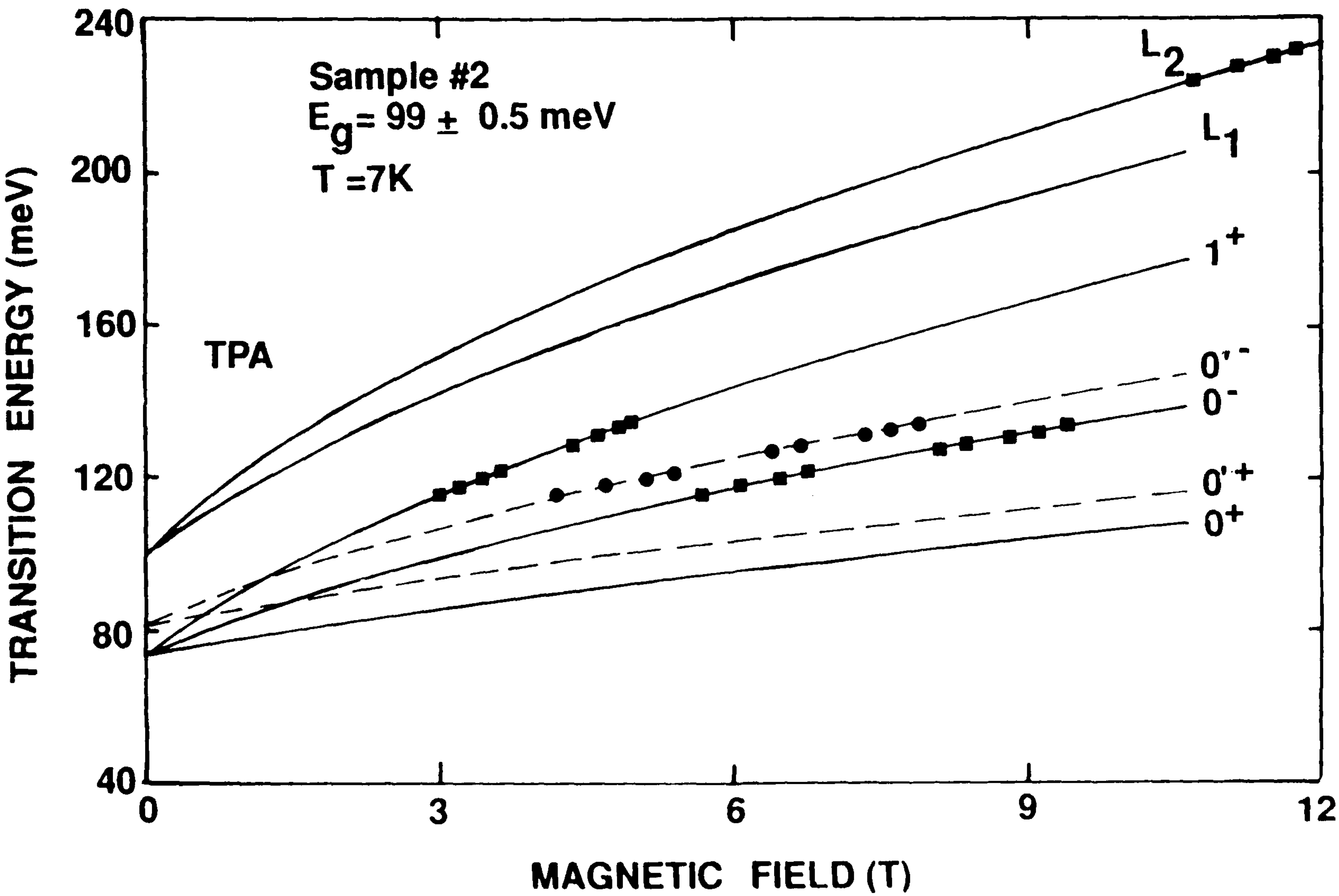

Figure 2. Fan chart plots of transition energy vs magnetic field showing TPA and deep acceptor impurity levels for sample 2. L_1 represents the two- photon transition $a^+(-1) \rightarrow a^c(1)$ and L_2 the TPA transition $b^+(-1) \rightarrow b^c(1)$. The numbers at the end of the theoretical lines identify the final state conduction band Landau levels involved in the impurity transition, while the ± symbols represent the spin up and spin down magnetic states, respectively. The ′ symbol refers to a different charge state of the impurity.

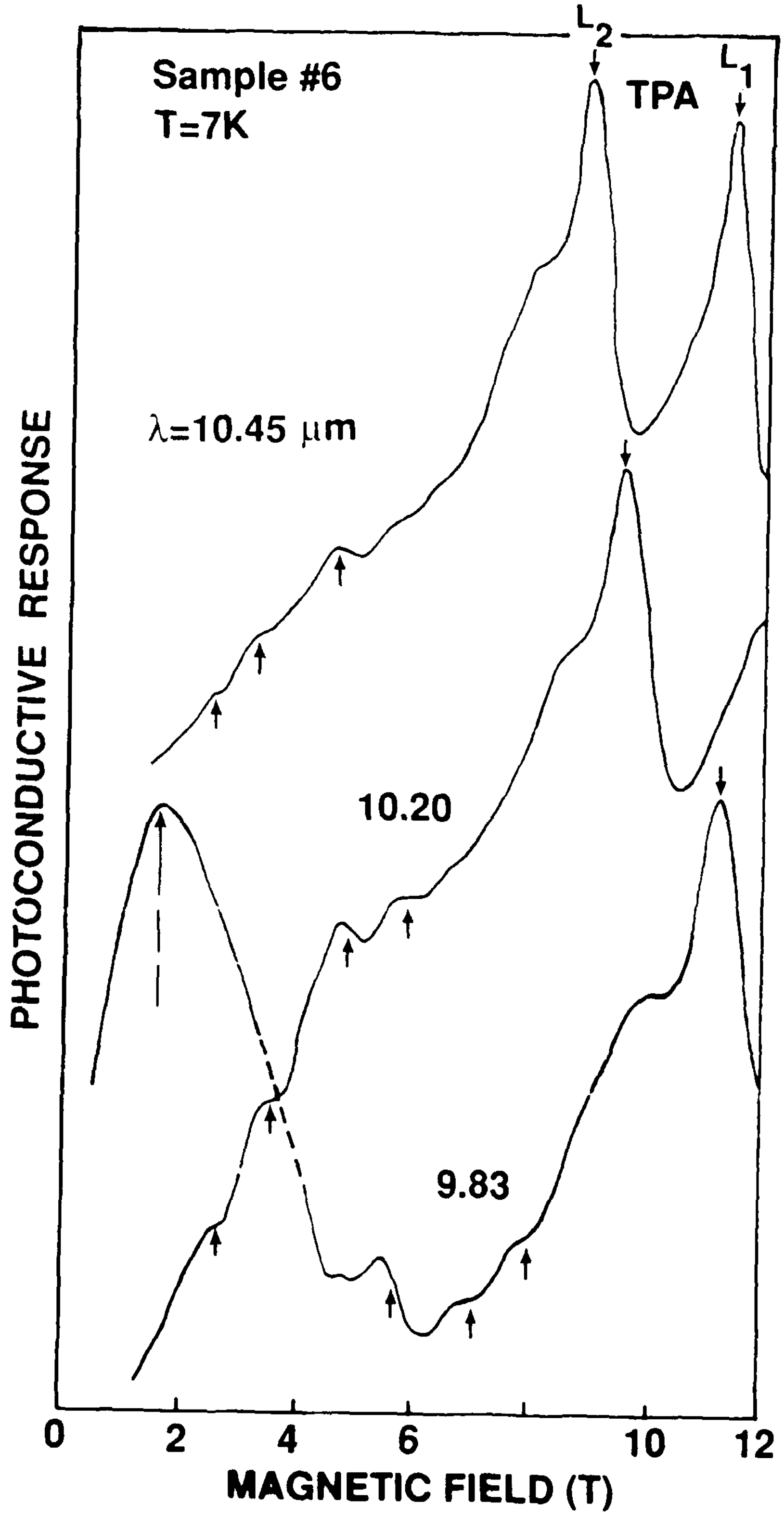

Figure 3. Wavelength dependence of the PC response for sample 6. The two large resonances at high field arise from TPA processes (downward arrows). The upward arrows indicate the magneto-optical resonances due to electron transitions from midgap levels to the conduction band.

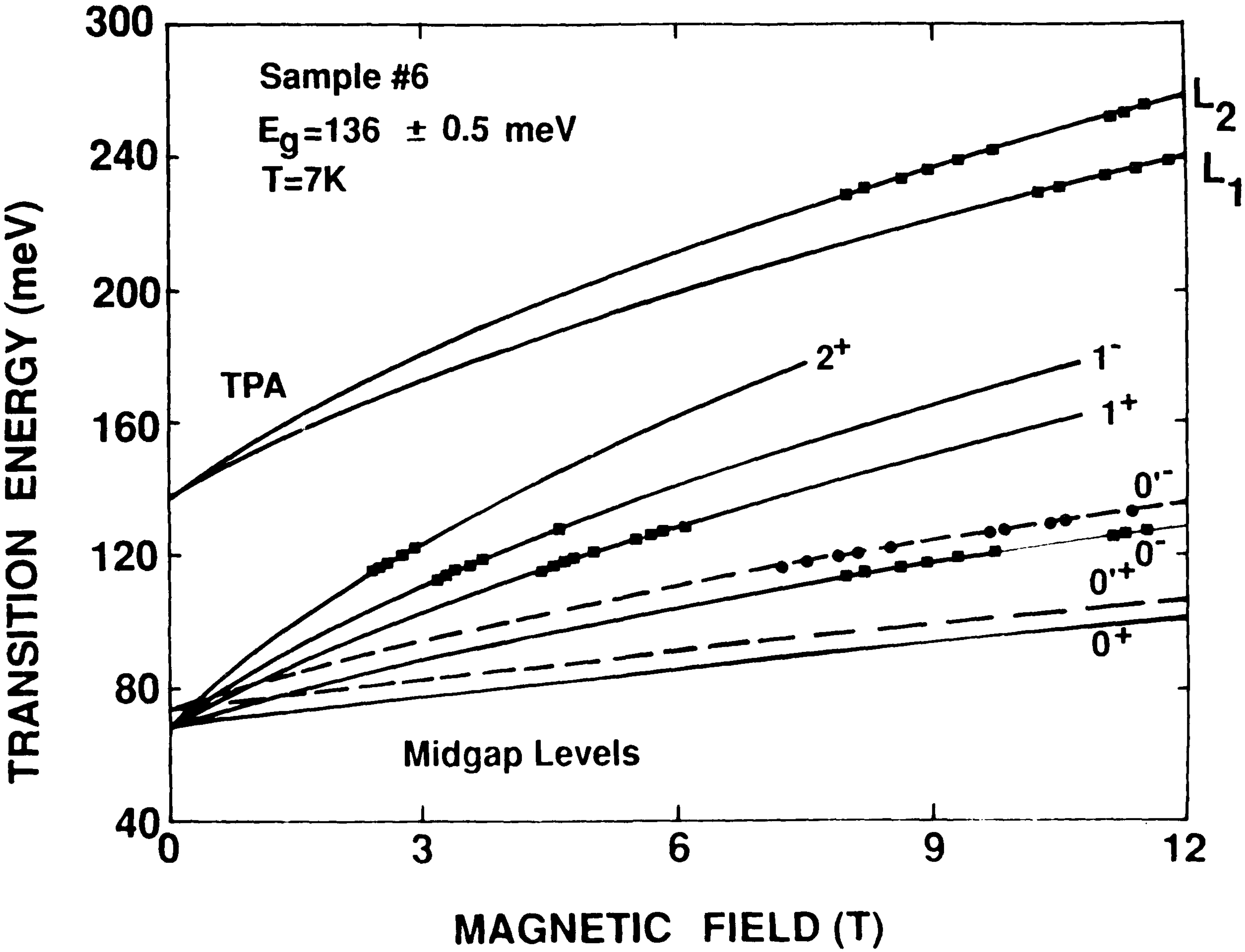

Figure 4. Transition energy vs magnetic field showing TPA and midgap level transitions for sample 6.

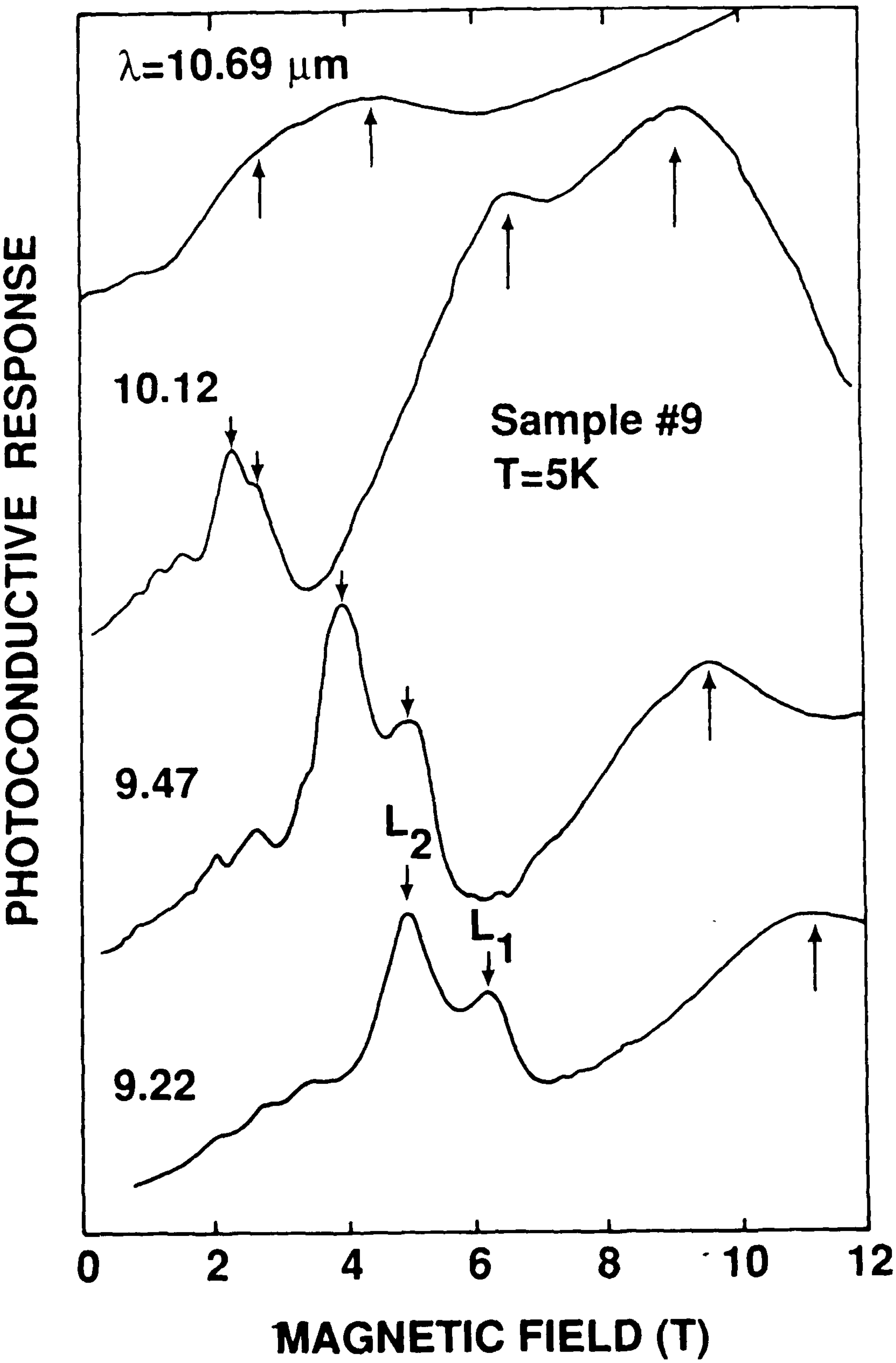

Figure 5. Magneto-optical spectra for sample 9 showing TPA structure (downward arrows) and midgap level to conduction band transitions (upward arrows).

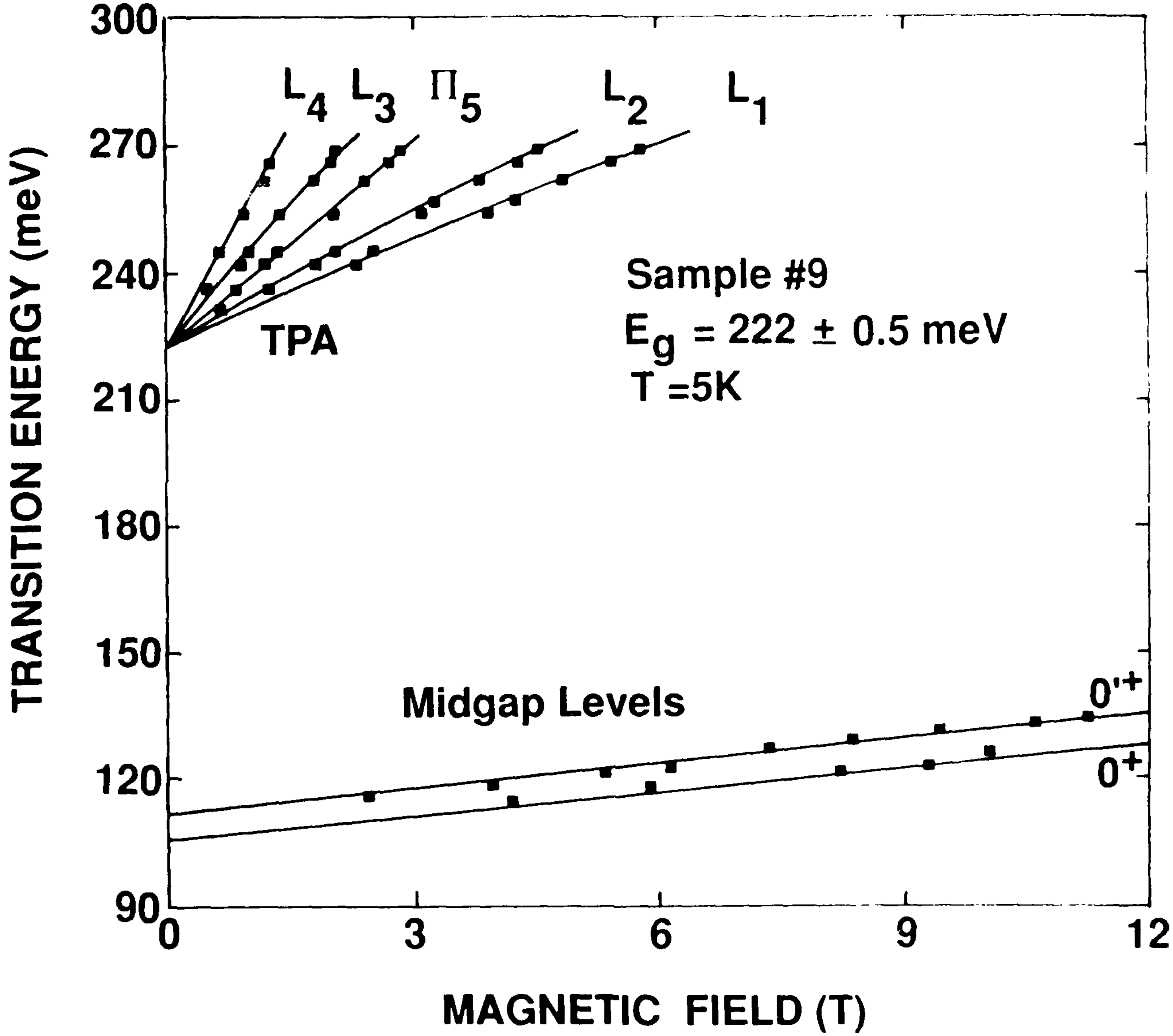

Figure 6. Transition energy vs magnetic field for sample 9. The activation energies of midgap levels determined from the zero-field intercepts are 111.5 and 116 meV above the valence band.

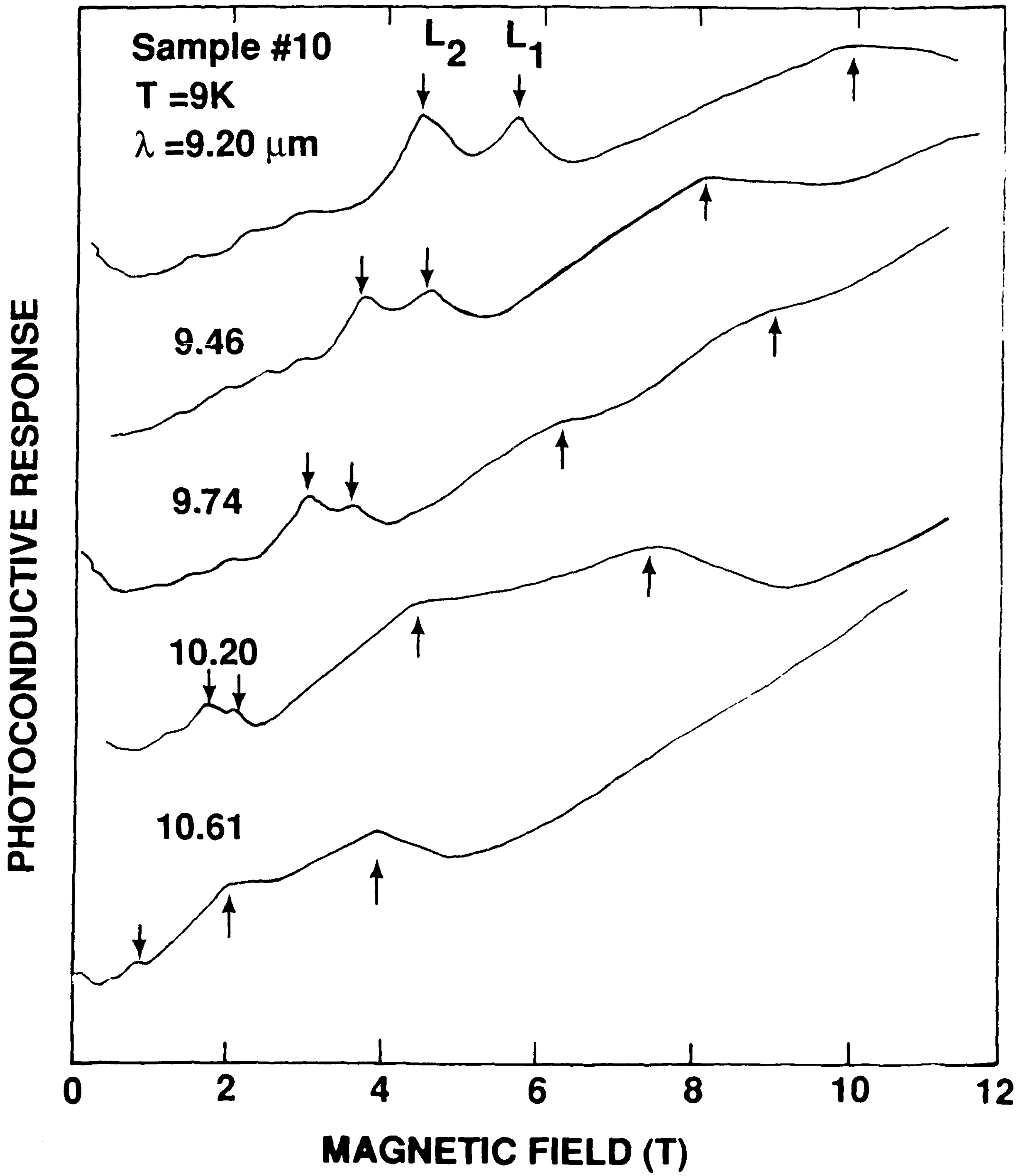

Figure 7. Wavelength dependence of the PC response for sample 10 (p-type). Upward arrows represent transitions from midgap levels to the conduction band and downward arrows indicate TPMA resonances.

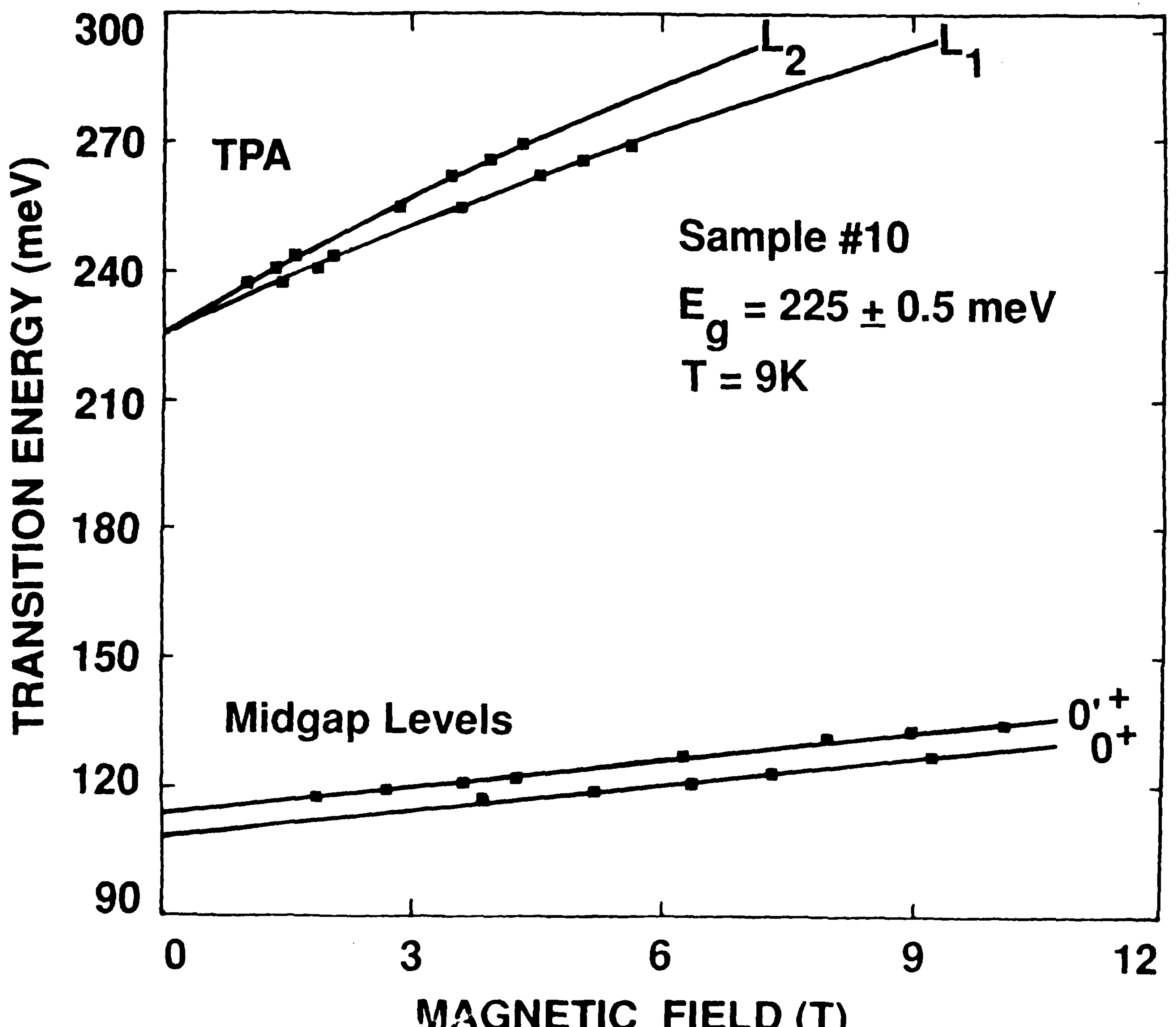

Figure 8. Transition energy vs magnetic field showing TPA and midgap level transitions for sample 10.